

SHS EXTRUSION OF ELECTRODE MATERIALS AND THEIR APPLICATION FOR ELECTRIC-SPARK ALLOYING OF STEEL SURFACES

V. V. Podlesov, A. M. Stolin, and A. G. Merzhanov

UDC 621.9.048

A method of SHS extrusion, allowing production of electrodes for electric-spark alloying from a variety of materials, is described. The properties and the microstructure of the obtained materials and applied coatings are studied. Results of testing the service characteristics of coatings are presented, among them those of industrial trials of a hardened tool.

Introduction. One of the methods currently most widely used for hardening metal surfaces is electric-spark alloying (ESA), based on the principle of transfer of the anode material to the cathode in an electric discharge [1]. ESA is used most often for increasing the hardness and wear-resistance of the working surfaces of parts and tools. Here, the main advantages of the method reveal themselves in full measure, viz., the possibility of a local treatment of the surface only in the places of maximal wear, a high strength of cohesion of the applied material with the base, no heating of the part during alloying, and no need for its preliminary preparation and subsequent mechanical treatment. Moreover, ESA is used to apply corrosion- and heat-resistant coatings, to reduce the friction coefficient of the surfaces, to restore the sizes of the worn parts, and for other purposes [2].

Among the important factors governing the technical advance of the method we may distinguish the assurance of commercial production of electrodes from a variety of materials based on refractory compounds. At present, commonly used units for ESA come complete with the electrodes made of hard alloys based on tungsten carbide of grades VK and TK. The familiar methods for producing electrode materials employ the traditional techniques of powder metallurgy, viz., pressing and vacuum sintering or hot pressing [3]. These technologies involve a great number of operations, many of them complicated, energy-intensive, and long-run.

The technological difficulties make themselves most evident in fabricating electrodes of small diameter (1-2 mm), which are widely used in automated units, especially, of ELFA type. To produce such electrodes, a plasticizer, e.g., a blend of beeswax and paraffin, is introduced into the powder mixture. From the plasticized mixture, by a cold die-pressing billets are shaped, which are subjected to annealing at a temperature of 100-300°C to remove the plasticizer. Afterwards, the billets are sintered at a temperature of 1400-1600°C in the vacuum for several hours. Here, with even insignificant deviations in the production modes or with temperature gradients in the furnace, there are cracks, axial bends, and other defects in the manufactured electrodes.

A novel approach, in principle, to implementing the technological process of producing electrodes is opened up by virtue of the application of SHS extrusion [4], owing to which their fabrication simplifies appreciably, synthesis of the material and shaping of the products are accomplished for several seconds (instead of hours) in a single technological cycle. This method permits fabrication of the electrodes from various hard-alloy materials based on carbides and borides of transition metals. The current study presents the method of SHS extrusion for electrode materials and the results of using them to apply protective coatings.

1. Specific Features of the Technological Process of SHS Extrusion for Electrodes. SHS extrusion consists essentially of carrying out a self-propagating high-temperature synthesis of the base product (in this case, a tungsten-free hard alloy) with a subsequent extrusion of the hot synthesized material through a die. Figure 1 shows the basic stages of the process.

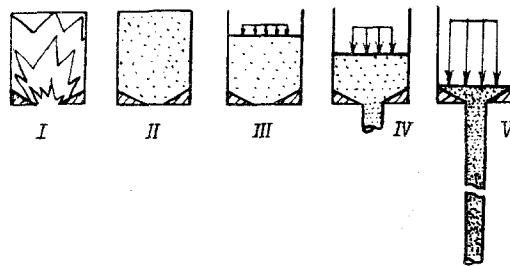


Fig. 1. Basic stages of SHS extrusion.

I. Ignition and combustion of the charge billet. A local heat pulse of length about 1 sec initiates a combustion wave, which propagates over the entire charge billet. The combustion time is governed by the combustion rate of the composition and by the billet height, and generally constitutes a few seconds. At this stage, the material synthesis from the original components and primary structurization processes occur.

II. Degassing and cooling of the burned billet. The removal of impurity gases, liberated in the combustion, terminates, and the base product reaction to completion and structurization proceed. The material cools from the combustion temperature to the extrusion temperature. The extrusion temperature is chosen lower than the melting point of the metal binder to prevent its volume redistribution during the extrusion. At the same time, the extrusion temperature must be consistent with the maximal plasticity of the material. The duration of this stage is determined by the billet mass and takes several seconds.

III. Compaction of the synthesized material. By the action of the press, product deformation occurs with closing of macropores and with persistence of the structurization processes, which have to do with the variation in grain sizes of the solid base.

IV. Billet extrusion through the die. The material is further compacted in the conic section of the die and extruded through it; in this case the shape and size of the electrodes produced are determined by the configuration of the exit section of the die. The extrusion rate, just as the compaction rate, is specified by the velocity of the press plunger and depends on the rheological properties of the material.

V. Cooling of the finished product. The extrusion is discontinued on the material having lost plasticity as a result of cooling (here, the nonextruded part of the material forms a press-residue) or after its complete extrusion. In the extruded product, the processes of grain growth terminate, and the length at the final stage is determined by the product size and heat-transfer conditions.

The SHS extrusion of the electrodes was conducted in the rig presented schematically in Fig. 2. The rig comprises a press (1), an extrusion mold (2), and a control unit (3). The process of producing the electrodes is accomplished as follows. The billet, premolded from the original charge and having a thermally insulated surface, is placed into the mold container, with a conic-shaped die and a punch located in its lower part, and a cover and an initiation device in its upper part. The mold thus assembled is placed under the press plunger. The ignition is effected via a tungsten spiral on command from the control unit. After the sample has burned and cooled to the extrusion temperature, the press turns on from a signal of the control unit, and the hot synthesized material is first pressed and thereupon extruded through the die. To ensure against axial bends of the electrodes, a guide gauge positioned in the inner channel of the duct is used. As a result, rods 1-5 mm in diameter and longer than 300 mm are obtained, which are then cut into standard electrodes of length 45 mm.

The workability of any technological method depends on the extent to which the properties of the articles produced are reproducible; therefore, it is important to specify the process parameters clearly. The present study paid much attention to the choice of key technological parameters for the SHS extrusion, which we believe are the mass of the original charge, the extrusion temperature, degree of deformation, pressure, extrusion rate, and the geometry of the pressing equipment. We have studied the effect of these parameters on the extrusion completeness and on the length and quality of the manufactured electrodes, which enabled us to determine the optimal values of the technological parameters.

The main requirements of the electrodes for ESA are a high homogeneity of the composition over the electrode length and cross section, as well as a uniform and fine-granular structure. We considered in detail the composition, properties (density, hardness, specific electric conductance, etc.), grain size of the electrodes, and their ranges at fixed parameters. The data obtained allow us to deduce that the process is highly reproducible, whereas the composition, microstructure, and properties are fairly stable both along the length and over the cross section of the electrodes.

TABLE 1. Some Characteristics of Electrodes Made of SHTM Alloys

Alloy grade	Solid base	Density, g/cm ³	Average grain size, μm	Hardness, HRA
SHTM-2/20N	TiC	5,56	5-6	80,5
SHTM-2/30N	TiC	5,8	3-3,5	79
SHTM-3/10N	TiC-Cr ₃ C ₂	5,37	3-4	92
SHTM-3/20	TiC-Cr ₃ C ₂	5,6	2-4	90
SHTM-4	TiB	4,2	1-2	86

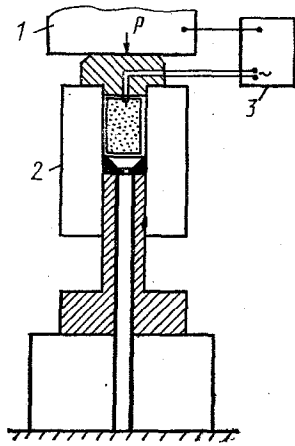


Fig. 2

Fig. 2. Schematic of the rig for SHS extrusion.

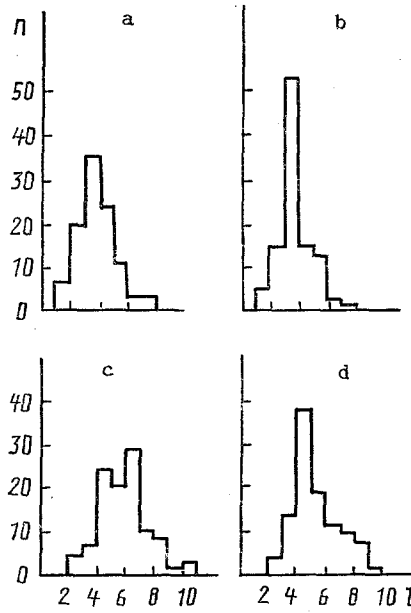


Fig. 3

Fig. 3. Size distribution of grains at the center (a, c) and over the periphery (b, d) of the cross section of electrodes: a, b) SHTM-2/30N; c, d) SHTM-2/20N; a) $l_{av} = 3.3 \mu\text{m}$; b) 3.2; c) 5.8; d) 5.2 μm . l , μm .

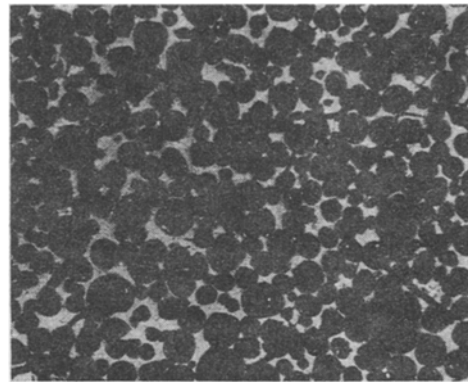


Fig. 4. Characteristic microstructure of electrodes made of SHTM-2/20N. $\times 1000$.

The average grain size slightly decreases from the center to the surface of the electrodes, and the uniform graininess of the structure also somewhat reduces in this direction (Fig. 3). These phenomena are likely the result of a more rapid cooling of the surface layers of the extruded electrodes.

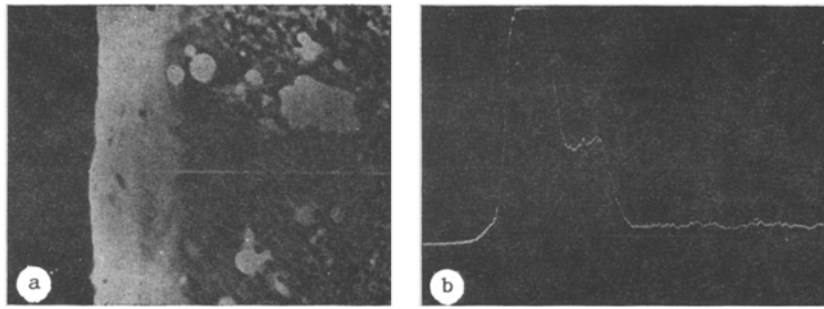


Fig. 5. Microstructure of a steel surface hardened by an electrode made of SHTM-2/20N (a) and concentration profile of titanium in a hardened layer (b). $\times 2800$.

2. Compositions, Microstructure, and Properties of the Electrode Materials and Alloyed Layers. The selection of an electrode material determines the quality and the operational characteristics of the coatings produced. There are no universal electrode materials. In the cases when only the surface wear resistance is to be increased, the standard alloys VK and TK [5], and tungsten-free hard alloys [6] are widely applied. The electrodes fabricated using SHS extrusion from the alloys of SHTM (synthetic hard tool materials) proved to be quite competitive with the standard alloys, in some cases surpassing them in the wear-resistance of surfaces [8]. Introducing special dopes into the electrode materials may markedly improve the characteristics of the alloying process and the quality of the coatings [9]. A still more significant effect may be produced by creating new electrode materials for solving certain problems, for example, for applying coatings simultaneously corrosion- and wear-resistant [10], as well as heat-resistant and other coatings. Below we present a review of investigations on all these materials.

Electrodes Made of SHTM Alloys. Using SHS extrusion, electrodes are fabricated from a number of SHTM alloys, whose solid base is carbides and borides of transition metals. Table 1 gives some characteristics of the electrodes made of these alloys.

As an illustration, Fig. 4 shows the characteristic microstructure for the electrodes manufactured from SHTM-2/20N. The photographs made with a little magnification reveal that the electrodes have a residual porosity. In accordance with data [1], the porosity of the electrodes promotes their better erosion during ESA and, hence, increases the coefficient of the electrode material transfer to the hardened surface. With a greater magnification, the characteristic microstructure of the electrodes is visible, i.e., roundish grains of titanium carbide surrounded by a nickel binder. Figure 3 shows a TiC size distribution.

The principal condition for successful use of the electrodes produced is the possibility of using them to apply by them high-quality hardened layers. Criteria of the hardening quality are the thickness, roughness, and continuity of the coatings. The continuity of the alloyed layer is determined by the presence of uncoated surface sections and evaluated visually with the aid of a microscope. The coating thickness and roughness are dependent on the treatment mode and on the power of the devices employed.

The current strength, capacitance, pulse frequency, and specific time of the treatment are the ESA parameters affecting the quality of the hardened layer. The most influential for qualitative characteristics are the capacitance and the current strength, governing the amount of energy supplied to the working zone. With optimal alloying modes, continuous uniform layers generally of thickness 10-60 μm are produced (Fig. 5).

The coating is a white layer not etched by conventional metallographic methods. Data on its structure may be obtained using a x-ray microanalysis. Figure 5a presents a photograph of the steel surface hardened by an electrode made of SHTM-2/20N, with a line of scanning by an electric probe, and Fig. 5b gives a titanium concentration profile in the coating. The hardened layer is of intricate structure and consists of at least two zones. The titanium concentration and, therefore, the alloying degree in the surface zone of the coating are much higher than in the zone adjoining the substrate. This may be attributed to the fact that the surface zone constitutes the coating proper, whereas the lower zone has formed by diffusion of the electrode material into the substrate. Such a structure of the alloyed layers predetermines their good cohesion with the substrate. The coating microhardness for various electrode materials is as large as 11-19 GPa.

Electrode Materials with Dopes of a Datolite Concentrate. The electrode materials must be prepared taking into account that the ESA process proceeds mainly in air, which gives rise to the formation of brittle oxides and decreases the efficiency of the formation of the alloyed layer. To reduce the origination of oxide films on the surface of the alloyed layer, the components

TABLE 2. Composition and Some Characteristics of Electrodes

Electrode material	Composition, %			Porosity, %	Average grain size, μm	Hardness, GPa		
	TiC	Ni+Mo	DTC			H_{μ}^{200} total	H_{μ}^{50} of grain	H_{μ}^{20} of binder
D0	70	30	—	4—6	3,59	12,42	16,7	7,96
D1	70	29,5	0,5	6—7	3,13	10,85	16,42	9,77
D2	70	29	1	7—8	3,03	9,0	16,13	6,0
D3	70	28,5	1,5	8—10	2,54	9,2	23,03	—
D4	70	28	2	10—11	2,26	11,09	22,79	—

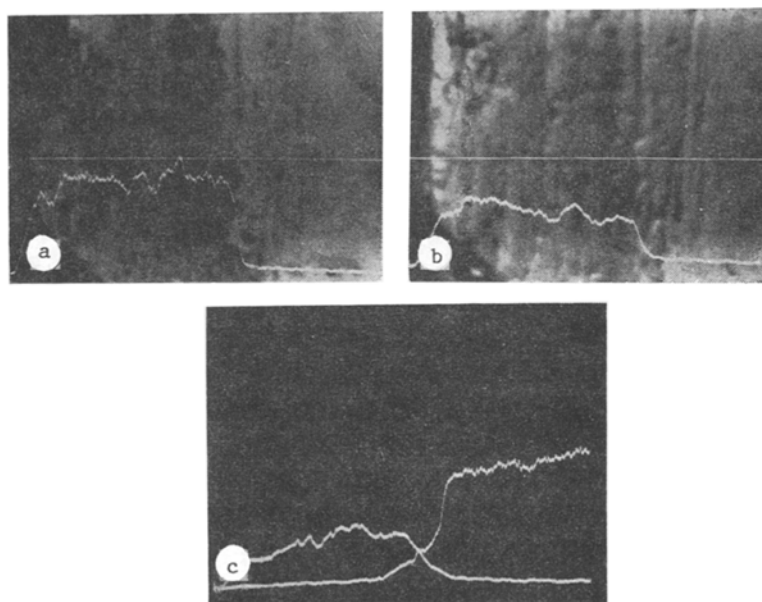


Fig. 6. Distribution of elements in a coating applied by the D3 electrode. $\times 1800$.

acting as fluxes (boron, silicon, phosphorus, manganese, and alkali metals) are usually introduced into the composition of the electrode material. Moreover, the introduction of boron is appropriate for decreasing the electric-erosion resistance of the materials [12].

Using pure initial components, in particular, boron, makes the production of electrodes more expensive. The requirements for purity of the starting material may frequently be lowered, and an ore starting material may be used. As an alloying dope, study [13] applied the datolite concentrate (DTC) CaB [SiO₄](OH) with the following chemical composition (percent by weight): 36.72 for SiO₂, 17.14 for B₂O₃, 37.12 for CaO, 2.05 for Fe₂O₃, 0.56 for FeO, 0.27 for MnO, 0.02 for TiO₂, 0.83 for Al₂O₃, 0.91 for MgO, 0.08 for Na₂O, 0.02 for P₂O₅, 0.1 for SO₃, and 4.44 for H₂O.

As the electrode material, a tungsten-free hard alloy based on titanium carbide with a nickel-molybdenum binder (with the ratio Ni:Mo = 3:1) was used. The selection of the material composition is not random; the familiar studies on producing electrode materials from tungsten-free alloys obtained the most homogeneous and wear-resistant layer by doping it with alloys containing 20-30% of a binder [6]. Table 2 gives compositions and some characteristics of the electrodes produced.

Clearly, the average grain size of carbide decreases with increasing content of datolite. This is, apparently, linked with the growing number of recrystallization centers during the high-temperature synthesis. Besides, a rise in the porosity of the electrodes is observed, which is due to an increase in the content of the oxide phase of the charge, playing the role of a frictional dope in the extrusion.

The total microhardness of the material diminishes slightly with increasing datolite content, which is connected with softening of the intergrain boundaries. Here, the microhardness of carbide grains grows, owing to their alloying with datolite components, primarily, with boron.

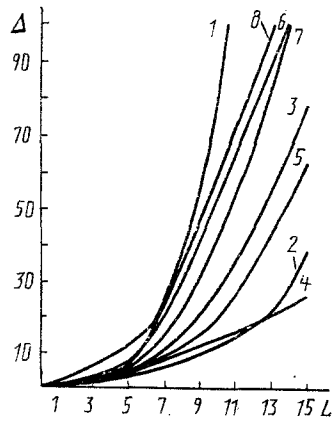


Fig. 7

Fig. 7. The wear Δ (μm) vs the creep distance L (km) for samples of steel Kh12F1 with coatings applied by the following electrodes: 1) D0; 2) D1; 3) D2; 4) D3; 5) D4; 6) D5; 7) D6 and D7; 8) SHTM-2/30N.

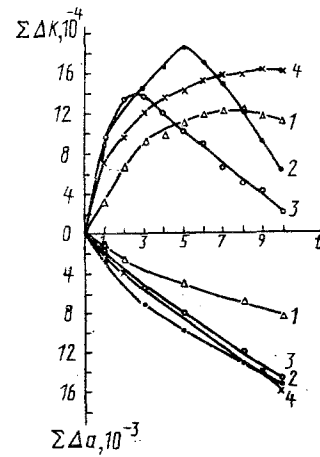


Fig. 8

Fig. 8. Dependence of the net erosion of the anode $\Sigma\Delta a$ (10^{-3} cm^3) and of the increase in the cathode weight $\Sigma\Delta k$ (10^{-4} cm^3) on the time of ESA t (min/cm^2) by the following alloys: 1) T2; 2) T4; 3) T5; 4) T6.

We considered the kinetics of alloying a steel surface with the materials produced, the time dependences for the specific and net erosion of the anode and for the increase in the cathode weight, and we found a threshold for the brittle fracture of the layer, the material transfer coefficient, and the ESA efficiency [14]. The materials D3 and D4 with 1.5-2% of datolite possess the best characteristics with respect to all of the parameters. This may be explained by an increase in the fraction of the electrode erosion in the liquid phase. With the datolite content rising to 3-5% (the materials D5-D7), the brittle fracture of the electrodes in electric-spark discharges increases in importance, and the ESA parameters are adversely affected.

The investigations demonstrated that a layer of thickness 20-60 μm and microhardness 9-13 GPa forms on the surface of the samples. Figure 6 shows photographs of a steel surface alloyed by the electrode D3, which were made using an x-ray microanalyzer in the compo (a) and topo (b) modes, with concentration profiles for Ti (a), Mo (b), and Ni and Fe (c). Such a pattern of the component distribution is bound up with specific features of the formation of the alloyed layer, exemplified by transfer of the anode material to the cathode, by generation of the zone of mutual crystallization, by diffusion of the anode elements into the cathode, and, vice versa, by diffusion of the base elements into the coating.

The key issue in studying the quality of coatings is their service characteristics, specifically, wear resistance. The wear resistance was investigated using a frictional machine connected in a shaft-block circuit, and the hardened steel 40Kh was taken to be the counterface material. Figure 7 plots the wear of alloyed samples vs the creep distance. The minimal intensity of the wear is observed on the coatings applied by the D1, D3, and D4 electrodes. The coatings applied by the electrodes with a higher content of datolite and those free from datolite wear out much faster.

Corrosion-Resistant Electrode Materials TaC-TiC-Kh18N9T. The industry faces in increasing frequency the problems of improving the wear resistance of parts operating in aggressive media. For these purposes, a corrosion-resistant material, based on a solid solution of tantalum carbides and titanium with a binder of steel Kh18N9T, was developed [15].

Table 3 shows the compositions and some characteristics of the manufactured electrodes. With increasing Ti fraction, the initial charge becomes more exothermal and the combustion temperature rises, and, consequently, the product is extruded more fully and its porosity decreases. An increase in the TiC content of the material contributes to its hardness; however, in this case the average size of the carbide grains is somewhat enlarged.

The corrosion resistance of the materials was determined through boiling in nitric and sulfuric acids of two different concentrations over 24 h. The mass fraction of the insoluble residue (in %) was calculated after the samples were weighed on a VLR-200 analytic balance. With decreasing TaC_{0.85} fraction in the material, its resistance to nitric acid diminishes insignificantly, whereas that to sulfuric acid increases (Table 4).

TABLE 3. Compositions and Some Characteristics of Electrodes

Electrode material	Charge composition, %				Calculated composition of material, %			Calculated composition of solid solution (Tam Ti)C, %		Density, g/cm ³	Average grain size, μm	Hardness, GPa
	Ta	Ti	C	Kh18N9T	TaC _{0,18}	TiC	Kh18N9T	TaC _{0,18}	TiC			
T2	39,8	22,4	7,8	30	42	28	30	60	40	7,7	1,9	13,5
T4	26,5	33,6	9,9	30	28	42	30	40	60	6,75	2,1	15,2
T5	13,2	44,8	12	30	14	56	30	20	80	6,23	1,8	14,5
T6	—	56	14	30	—	70	30	—	100	6,0	2,3	16,2

TABLE 4. Resistance of Electrodes to the Action of Nitric and Sulfuric Acids Electrode material

Electrode material	Insoluble residue after boiling for 24 h, %			
	HNO ₃		H ₂ SO ₄	
	74%	37%	96%	48%
T2	98,3	97,65	94,85	89
T4	95,5	97,3	93,3	96,9
T5	98,3	97,6	99	96,4
T6	96,9	95,8	98,4	96,5

TABLE 5. Results of Metallographic Analysis of Coatings

Electrode material	Continuity, %		Thickness, μm		Microhardness, GPa		
	2nd mode	3rd mode	2nd mode	3rd mode	of layer	HAZ*	of base
T2	50—60	to 100	5—10	to 30	12—13	4,2—4,5	3—3,2
T4	50—60	40—50	5—10	5—10	13—14	4,7—7,5	2,9—3
T5	40—50	40—50	20—30	20—30	13—16	5,6—6,7	3—3,1
T6	30—50	80—90	5—10	20—30	17—19	3—4	3—3,2

*Heat-affected zone.

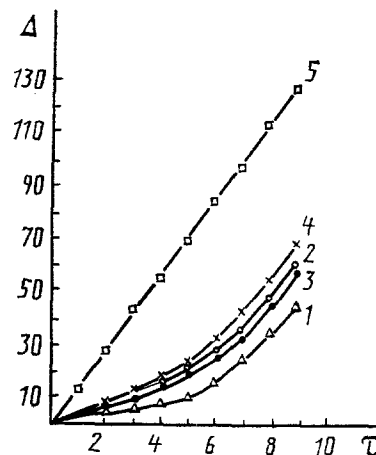


Fig. 9. The wear Δ (μm) of the samples with coatings on the steel 12Kh18N10T as a function of the time τ (min) of tests: 1) T2; 2) T4; 3) T5; 4) T6; 5) steel 12Kh18N10T.

Electric-spark alloying by the electrodes produced was executed using the Elitron-22A industrial unit in four modes. Stainless steel 12Kh18N10T and the titanium alloy VT1 were used as a substrate.

TABLE 6. Results of Testing a Hardened Tool

Tool	Material			Resist- ance increase	Enterprise
	of tool	of electrode	treated		
Shank cutter	R 6M5	SHIM -2/20 N	35 KhGSa	2,0	Plant "Kommunar," Moscow
Drawer	R 18	SHIM -2/20 N	30 KhGSa	1,6-2,0	
Cutter:					Plant "Nauka," Moscow
face-and-side	R 6M5	SHIM -3/20 N	U8, KhVG	1,5-2,5	
face-and-side	R 6M5	SHIM -3/20 St	U8, KhVG	3,0-5,0	
face-and-side	R 6M5	SHIM -4	U8, KhVG	2,0-3,5	
face-and-side	R 6M5	SHIM -2/30 N	U8, KhVG	3,0-4,0	
face-and-side	R 6M5	SHIM -4	VT8	1,5	
face-and-side	R 6M5	SHIM -3/20 N	VT8	1,5	
face-and-side	R 6M5	SHIM -3/20 St	VT8	1,5-2,0	
face-and-side	R 6M5	SHIM -2/30 N	VT8	1,5-2,0	
Drawer	R 18	SHIM -3/20 St	Steel 45	1,9	SMPO, Samara
Drill	R 6M5	SHIM -2/30 N	Steel 40	1,3	
Drill	R 6M5	SHIM -2/20 N	AKM	2,7	VNITI, St. Peters- burg
Drill	R 6M5	SHIM -2/20 N	24 Sh	2,0	
Shank cutter	R 6M5	SHIM -2/20 N	AKM	2,25	
Shank cutter	R 6M5	SHIM -2/20 N	24 Sh	1,7	
Needle for draw- ing dies	U8, U10	SHIM -2/30 N	VKZM	2,0-3,3	BMZ, Zhlobin
Bed knife	6KhV2S	SHIM 2/30 N	VKZM	10-12	
Knife:					
for cutting	6KhV2S	SHIM -2/30 N	Steel St3,70	3-8	
tubular	6KhV2S	SHIM -2/30 N	Steel St3,70	2,0-2,7	
figured	6KhV2S	SHIM -2/30 N	Steel St3,70	1,5-2,0	
Roller	40KhNMF	SHIM -3/20 St	Steel St3,70	1,5-2,0	
Slotting tool	R 18	SHIM -3/20 St	Steel 45	10-13	

TABLE 7. Results of Comparative Testings of Cutting Plates Treated Material Is ÉI698 (KhN73MBTYu)

Plate material	Electrode material	Cutting rate, m/min	Cut length, mm	Wear of back surface, mm	Resist- ance increase
EP688	Unhardened VK6M	9,5	35	0,4	—
(R9M4K8)	SHIM-3/10N		45	0,2	2,6
EP682	Unhardened VK6M		45	0,25	2,0
(R12F3K10M3)	SHIM-3/20St	11,4	5	1,0	—
	SHIM-4		15	1,0	3,0
	SHIM-2/20N		40	0,6	13,6
			18	1,05	3,6
			9	0,8	2,2

Figure 8 shows the kinetic relations for the net erosions of the cathode and for increases in the cathode weight with the third mode ($I = 1-1.4A$) for all materials studied. The maximal overall increase in the cathode weight is attained by doping with the alloy T4. The ESA efficiency and the transfer coefficient are maximal for the alloy T2.

The quality of the alloyed layers formed was checked by metallographic analysis for their continuity, thickness, and microhardness (Table 5). The investigations showed that a layer of thickness up to $30 \mu m$ and continuity up to 100%, with the hardness exceeding 4-6 times the substrate hardness, forms on the surface of the samples.

With increasing TiC content of the electrode material, the microhardness of the coatings is enhanced, which is in good agreement with the hardness of the material proper. The third mode can be regarded as optimal, since with this mode the layer has maximal continuity and thickness, whereas, with the fourth mode, burns of the alloyed surface start manifesting themselves.

TABLE 8. Results of Comparative testings of Cutters. Cutter Material R6M5, Treated Material 07Kh16N6

Electrode material	Resistance increase
Without hardening	1
KNT-16	5—6
SHTM/20st	8—9

The wear-resistance of the coatings was studied on the basis of the shaft-block scheme, and the rollers, covered with a diamond-bearing layer with a bronze binder, were taken to be a counterface. The tests were conducted at a creep velocity of 1 m/sec and a load of 0.3 MPa.

Figure 9 shows the results of studying the wear-resistance of the coatings. Obviously, the wear rate for the coated samples is not constant. For the first 3-5 min, the wear is much less than that of uncoated steel samples. Further testing of the samples during the next 5-7 min leads to a complete attrition of the coating and to leveling of the wear rate with the unhardened steel. The coatings applied by the T2 electrode are the most wear-resistant, which might be related to the maximal continuity of these coatings.

The corrosion resistance of the coatings was studied through boiling in nitric acid (of concentration 37%). The coatings applied by the T2 and T4 electrodes had the best corrosion resistance, and those applied by the T5 and T6 electrodes had the worst corrosion resistance, which is consistent with the corrosion resistance of the electrodes proper (with reducing TaC fraction in the electrodes and coatings their resistance to HNO₃ decreases). Coating with the alloy T2 may be recommended for improving the wear resistance of the parts operating in aggressive media, specifically, those containing bearing nitric acid.

3. Practice of Applying SHS Electrodes. The ultimate evaluation of the workability of the alloyed layer can be obtained only from industrial trials of the hardened parts and tools. The decisive factor in selecting the electrode material is generally assumed to be the specific service conditions for the parts, particularly, for their working surfaces, viz., the character of loads, cutting rate, temperature, and treated material.

Various national enterprises performed industrial trials, whose results are given in Table 6 [8, 16]. The derived data are indicative of the high service properties of the coatings applied via the SHS electrodes.

It is important to perform comparative resistance testings of a tool hardened by the SHS electrodes and by the standard hard alloys. Such testings were carried out at the Chernyshev MMPO on cutting plates (Table 7) and at the VNII Kompessor-mash on shank cutters (Table 8). The testing results point to the benefits of the SHS electrodes, which can be quite significant for the alloy SHTM-3/20 St.

Conclusion. The introduction discussed some advantages of SHS extrusion over traditional methods employed in powder metallurgy, in particular, an appreciable reduction in the number of labor- and energy-intensive operations. Considering the outcome of the investigations, we may also infer other benefits of this method.

The path from conceiving the idea of a new electrode material to realizing it and obtaining the product is markedly shortened. This is because of the number of operations of the technological cycle for manufacturing the electrodes, only one stage is to be optimized, namely, the SHS extrusion itself. The selection of modes for other operations does not present difficulties.

One more advantage of the method is linked with the requirements of the purity and quality of the initial powder materials. For SHS extrusion, this point is not as crucial as in powder metallurgy because the combustion process lessens these requirements. For now, it is difficult to predict the scope and prospects of SHS extrusion. Considering the indicated benefits, the method may be assumed to have all the prerequisites for effective use in industry.

LITERATURE CITED

1. A. D. Verkhoturov and I. M. Mukha, Technology of Electric-Spark Alloying of Metal Surfaces [in Russian], Kiev (1982).
2. A. E. Gitlevich, V. V. Mikhailov, N. Ya. Parkanskii, and V. M. Revutskii, Electric-Spark Alloying of Metal Surfaces [in Russian], Kishinev (1985).
3. I. M. Mukha, Hard Alloys in Small-Scale Production [in Russian], Kiev (1981).

4. A. G. Merzhanov, A. M. Stolin, V. V. Podlesov, et al., Method of Producing Articles from Powder Materials and Device for Its Implementation. International inventor's application WO90/07015 of June 28, 1990.
5. E. Ya. Ulitskii, Poroshk. Metall., No. 10, 34-39 (1976).
6. M. S. Koval'chenko, A. V. Paustovskii, S. N. Kirilenko, et al., Poroshk. Metall., No. 6, 47-50 (1984).
7. A. G. Merzhanov, Self-Propagating High-Temperature Synthesis: Twenty Years of Search and Findings. Preprint [in Russian], ISMAN, Chernogolovka (1989).
8. V. V. Podlesov and A. M. Stolin, Élektron. Obrab. Mater., No. 5, 66-68 (1991).
9. T. A. Sheveleva, A. D. Verkhoturov, S. V. Nikolenko, et al., Élektron. Obrab. Mater., No. 1, 26-30 (1991).
10. V. V. Podlesov, T. A. Sheveleva, A. E. Kudryashov, et al., Élektron. Obrab. Mater., No. 3, 16-24 (1992).
11. A. D. Verkhoturov, M. S. Koval'chenko, et al., Poroshk. Metall., No. 8, 35-39 (1983).
12. I. M. Mukha, A. D. Verkhoturov, and S. V. Gnedova, Élektron. Obrab. Mater., No. 4, 24-27 (1990).
13. T. A. Sheveleva, A. D. Verkhoturov, M. V. Inadze, et al., Élektron. Obrab. Mater., No. 5, 17-21 (1990).
14. A. D. Verkhoturov, I. A. Podchernyaeva, L. F. Pryadko, et al., Electrode Materials for Electric-Spark Alloying [in Russian], Moscow (1988).
15. T. I. Shishkina, V. V. Podlesov, and G. N. Komratov, Poroshk. Metall., No. 7, 18-24 (1992).
16. M. V. Inadze, N. A. Busel, V. V. Podlesov, et al., Vestsi Akad. Nauk BSSR, Ser. Fiz. Tekh. Navuk, No. 2, 13-16 (1991).